Environ. Sci. Technol. **1998**, *32,* 2865−2870

Experimental and Theoretical Treatment of Elementary Ligand Exchange Reactions in Aluminum Complexes

BRIAN L. PHILLIPS,[†]
JOHN A. TOSSELL,[‡] AND
WILLIAM H. CASEY*,[§]

Department of Chemical Engineering and Materials Science, Department of Land, Air and Water Resources, and Department of Geology, University of California, Davis, California 95616, and Department of Chemistry, University of Maryland, College Park, Maryland 20742

Substitution of a hydroxide or fluoride ion for a water molecule in the inner-coordination sphere of $Al(OH_2)_6^{3+}$ considerably weakens bonds from aluminum to other water molecules that are also in the inner-coordination sphere. The labilizing effect of these substitutions on the rate of dissociation of Al−O bonds is a model for ligand-promoted dissolution of aluminum (hydr)oxide minerals. Here measured activation parameters for ligand exchange are compared with ab initio calculations of the energetics for comparable reactions. Because solvent exchange is an elementary reaction, it is particularly well-suited for such comparisons. The calculations indicate that substitution of hydroxide or fluoride ion into the inner-coordination sphere greatly reduces the energy required to remove a water molecule. The calculated and measured activation energies, however, differ significantly. A reasonable interpretation is that interactions between hydration waters and second-sphere water molecules, which are usually partly or fully excluded from the calculations, contribute to the exchange mechanism.

Introduction

One legacy of Werner Stumm's work is some of our current *vocabulary* of geochemistry. We now routinely discuss the removal and addition of mass at mineral surfaces in terms of ligand-exchange reactions, with a glossary derived from solution-state chemistry. The analogy between dissolved and surface complexes is close and useful. As a mineral dissolves, oxygens linking a surface metal to the bulk structure are replaced by other ligands, such as water molecules. Ultimately, a complex detaches from the mineral as the last bridging oxygen is exchanged, usually after protonation. The total number of ligands around the metals is usually, but not always, conserved.

There are as yet no spectroscopies capable of probing rates and mechanisms of these surface reactions, but one promising approach is to use molecular orbital theory to calculate properties of proposed surface complexes. This field is advancing rapidly, but the calculations, when applied to disequilibrium, really provide rate information about *elementary* reactions—those that proceed as written on the molecular scale. The extent to which such calculations are quantitatively useful is unclear, because there are no experimental data for the rates of elementary aqueous surface reactions that can be compared with theoretical predictions. However, analogous reactions involving dissolved species provide examples by which experimental and theoretical results for elementary reactions can be compared.

One of the simplest reactions is replacement of one water molecule in the inner-hydration sphere of an aquo complex with a solvent molecule:

$$Al(OH_2)_6^{3+}(aq) + H_2O^* \leftrightarrow Al(OH_2)_5(^*OH_2)^{3+}(aq) + H_2O \quad (1)$$

There is no net Gibbs energy driving this reaction, but its rate can be measured at a state of dynamic equilibrium by ^{17}O NMR methods (see below). Furthermore, the rate changes when waters of hydration are replaced by other stable ligands in the inner-coordination sphere

$$AlL(OH_2)_5^{2+}(aq) + H_2O^* \leftrightarrow AlL(OH_2)_4(^*OH_2)^{2+}(aq) + H_2O \quad (2)$$

making this process particularly suited for molecular orbital interpretation. Rate data for complexes with $L = F^-$ and OH^- have been recently measured (*1, 2*) and are compiled in Table 1. As one can see, the labilizing effects of these ligands are large and progressive.

The ^{17}O NMR Method of Experimental Rate Measurements

The rate parameters compiled in Table 1 were measured by the dynamic ^{17}O NMR line-broadening technique, which has been described elsewhere (*1, 2, 23*−*28*). Here we give a brief review of this technique as applied in cases in which more than one complex exists in solution. The ^{17}O NMR transverse relaxation rate ($1/T_2$) of the H_2O in aqueous complexes contain a contribution from the exchange of water molecules between the inner-hydration sphere and bulk solvent. This exchange can be treated as a two-site process (see ref *3*), simplified by the condition that the exchange rate is small compared to the width of the ^{17}O NMR peak for the solvent water. Experimentally, the bulk water resonance can be broadened beyond detection by addition of paramagnetic Mn(II) to the sample, leaving only peaks for bound hydration waters. The T_2 values for these hydration waters are obtained from the NMR line widths, $T_2 = 1/\text{fwhm}\cdot\pi$, where fwhm is the full width at half-maximum peak height.

Two principal processes contribute to the T_2 relaxation constant of the ^{17}O nuclei in these hydration waters: (i) chemical exchange of oxygen between the complex and the solvent, which is characterized by τ, the mean lifetime for a water molecule in the inner-coordination sphere; and (ii) intrinsic nuclear magnetic relaxation having time constant $[T_2(q)]$, due to modulation of the coupling of the nuclear quadrupole moment to the electric field gradient by molecular motions. The observed relaxation rate is a sum of the component rates:

$$\frac{1}{T_2} = \frac{1}{\tau} + \frac{1}{T_2(q)} \quad (3)$$

The pseudo-first-order water-exchange rate coefficient, k_{ex}

* Corresponding author phone: (916)752-3211; fax: (916)752-1552; e-mail: whcasey@ucdavis.edu.
[†] Department of Chemical Engineering and Materials Science.
[‡] Department of Chemistry.
[§] Department of Land, Air and Water Resources and Department of Geology.

S0013-936X(98)00224-7 CCC: $15.00
Published on Web 08/29/1998

TABLE 1. Rate Coefficients for Exchange of Water Molecules from the Inner-Coordination Sphere of Al(III) Complexes to the Bulk Solution

species	k_{ex}^{298} [a] (s^{-1})	$\Delta H^{\ddagger}$ [b] (kJ mol^{-1})	$\Delta S^{\ddagger}$ [b] (J K^{-1} mol^{-1})	source
$Al(OH_2)_6^{3+}$	1.3	81−85	42	30
$Al(OH_2)_5F^{+2}$	111 (±0.14)	79 (±5)	60 (±8)	1
$Al(OH_2)_4F_2^{+}$	19 600 (±0.05)	69 (±5)	70 (±17)	1
$Al(OH_2)_5(OH)^{2+}$	31 000 (±0.25)	36.4 (±5)	−36.4 (±15)	2

[a] Estimated standard deviations are reported for $\ln(k_{ex}^{298})$, not k_{ex}^{298}, and were obtained by propagating a 10% uncertainty in the linewidths through fits to eqs 3−5. [b] Uncertainties are reported as an estimated standard deviation of the mean.

(s^{-1}), is the inverse of the average lifetime of the water molecules in the complex, and its temperature dependence takes the form

$$k_{ex} = \frac{1}{\tau} = \frac{k_b T}{h} e^{\Delta S^{\ddagger}/R} e^{-\Delta H^{\ddagger}/RT} \quad (4)$$

where the exponential terms include the activation entropy [$\Delta S^{\ddagger}$] and activation enthalpy [$\Delta H^{\ddagger}$] for chemical exchange. The parameters k_b, T, R, and h are Boltzmann's constant, temperature in Kelvin, the gas constant, and Planck's constant, respectively. An Arrhenius-like relation is used to approximate the quadrupolar relaxation

$$\frac{1}{T_2(q)} = W_{q,298} e^{(E_q/R)[(1/T) - (1/298)]} \quad (5)$$

where $W_{q,298}$ is the value of $1/T_2(q)$ at 298 K and the term E_q is an activation energy for the motions that cause quadrupolar relaxation.

To obtain accurate values for the activation and rate parameters for chemical exchange, it is usually necessary to measure T_2 over as wide a temperature range as possible and fit the resulting temperature dependence to eqs 3−5. Due to the contrasting motional regimes of chemical exchange and quadrupolar relaxation, the value of T_2 observed for the bound waters in any given complex typically goes through a maximum as a function of temperature. Chemical exchange dominates T_2 in the high-temperature regime, and the quadrupolar relaxation dominates at low temperatures. For example, at room temperature water exchange for $Al(OH_2)_6^{3+}$(aq) is slow on the NMR time scale and the ^{17}O NMR line width of bound water reflects primarily the quadrupolar relaxation rate. Chemical exchange dominates the ^{17}O line width of bound waters at temperatures above ~260 K. Therefore, the uncertainty in the value of k_{ex}^{298} for this complex arises largely from the extrapolation of high-temperature line widths, where the quadrupolar contribution is very small, to 298K.

Water molecules in the inner-coordination sphere of Al(III) complexes give ^{17}O NMR peaks near +22 ppm and their chemical shift does not appear to change significantly when other ligands are substituted for adjacent inner-sphere waters. Thus, the peaks for hydration waters in different Al(III) complexes overlap. Measurement of T_2 in such cases depends on the lifetime of the complexes relative to τ, which can be divided into two limiting cases: (1) kinetically stable complexes, for which the lifetime of the complex is long compared to τ; and (2) short-lived complexes that exist for a time short compared to the lifetime for water in the inner-coordination sphere.

The resonances for hydration waters in different kinetically stable complexes can be resolved from one another at temperatures where their T_2 values differ sufficiently that a non-Lorentzian peak occurs as a result of superposition of

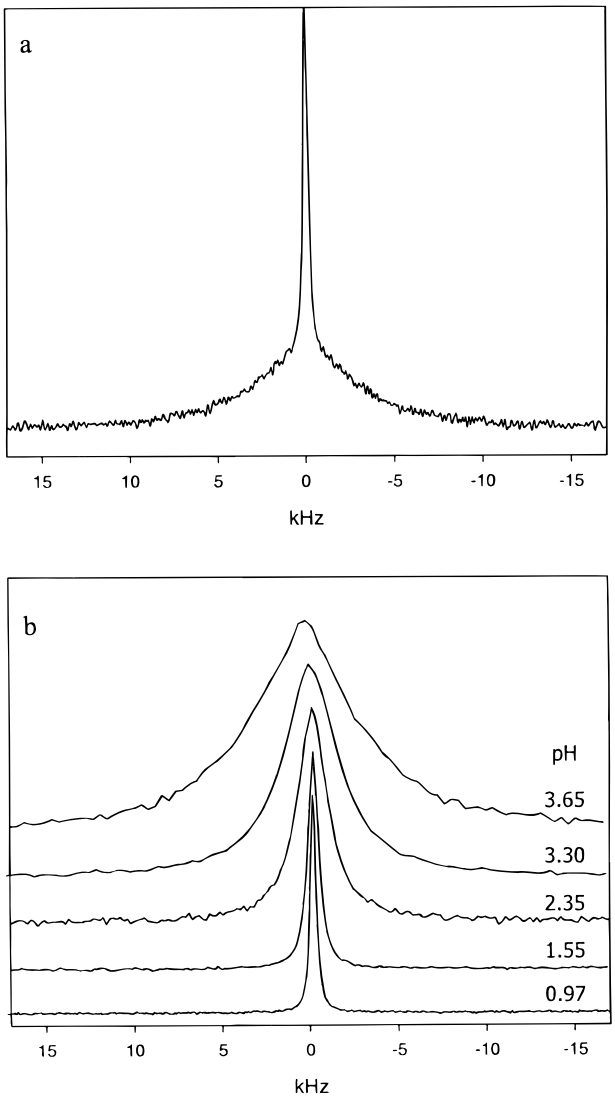

FIGURE 1. (a) ^{17}O NMR spectrum of 0.1 m $AlCl_3$ solution containing 0.1 m NaF and 0.25 m $MnCl_2$, taken at 83 °C. The broad component arises from bound waters in $AlF(OH_2)_5^{2+}$, which exchange rapidly with solvent, and the narrower component from the more slowly exchanging waters in $Al(OH_2)_6^{3+}$. (b) ^{17}O NMR spectra taken at 90 °C for various pH values, which were measured at 298 K. The solution consists of 0.1 m $AlCl_3$ and 0.25 m $MnCl_2$. The peak width is related to the concentration of the first hydrolysis product, which exhibits fast water exchange and interconverts rapidly with $Al(OH_2)_6^{3+}$ (eq 7). Origin of the frequency scale is arbitrary.

broad and narrow components (Figure 1a). Each of the superposed components corresponds to hydration waters in a different complex. In a solution containing $AlF(OH_2)_5^{2+}$(aq) and $Al(OH_2)_6^{3+}$(aq), for example, T_2 values for each complex can be obtained at higher temperatures by fitting the observed ^{17}O NMR spectrum to a sum of two peaks to give line widths for each component. Near room temperature, however, the quadrupolar contribution dominates the ^{17}O NMR line width of these complexes but does not differ enough between them to allow separate components to be resolved. Thus, some uncertainty in the activation parameters arises because of the difficulty in determining the increasing contribution of $T_2(q)$ with decreasing temperature.

The complexes $Al(OH_2)_6^{3+}$(aq) and $AlOH(OH_2)_5^{2+}$(aq) interconvert via proton exchange with bulk waters, which is very rapid relative to rates of water exchange from the hydration spheres. For solutions containing only these

complexes, a single ^{17}O NMR resonance is observed for hydration waters (Figure 1b). The line width of this single ^{17}O NMR resonance is proportional to the sum of the rates of water exchange for each species [$Al(OH_2)_6^{3+}$(aq) and $AlOH(OH_2)_5^{2+}$(aq)], weighted by their relative concentrations.

The temperature dependence of the composite line width can be fit to eqs 3−5 to yield an apparent rate coefficient. If only the $Al(OH_2)_6^{3+}$(aq) and $AlOH(OH_2)_5^{2+}$(aq) complexes are important, this apparent rate coefficient should vary linearly with $[H^+]^{-1}$ [or $AlOH(OH_2)_5^{2+}$(aq) concentration]

$$k^T_{ex,obs} = k^T_1 + k^T_2 [H^+]^{-1} \quad (6)$$

where k^T_1 is the rate coefficient for exchange of inner-sphere water molecules with bulk solution for $Al(OH_2)_6^{3+}$(aq) [$k^T_{ex,Al(H_2O)_6^{3+}}$], $k^T_2 = k^T_{ex,AlOH(H_2O)_5^{2+}} \cdot K^T_{a1}$, and K^T_{a1} is the first hydrolysis constant:

$$Al(OH_2)_6^{3+} \leftrightarrow AlOH(OH_2)_5^{2+} + H^+ \quad (7)$$

The validity of eq 6 was confirmed experimentally (*2*), and activation parameters for exchange of water from $AlOH(OH_2)_5^{2+}$(aq) were obtained from fits to the temperature dependence of $k^T_{ex,AlOH(H_2O)_5^{2+}}$ using eq 4.

Computational Methods

Modern quantum chemical methods are able to reproduce reaction energies to chemical accuracy (4−8 kJ mol^{-1}) for small molecules composed of light atoms in the gas phase (e.g., refs *4* and *5*). The basic procedure for gas-phase reactions is to solve an approximate version of the Schrodinger equation, typically the Hartree−Fock or Kohn−Sham equation, to high accuracy. A general problem is that mean-field procedures such as the Hartree−Fock method, in which the instantaneous electron−electron repulsion is replaced by an averaged value, can give serious errors in energies unless the reaction is of a specific, limited type in which the numbers and types of bonds are very similar in reactants and products. Corrections to the "correlation" error must generally be made to get accurate energies. A computationally efficient correction method is second-order Møller−Plesset perturbation theory (MP2; *6*).

Evaluating the energetics of reactions in solution is much more difficult, but it is a current focus of interest in quantum chemistry (e.g., refs *7* and *8*). For such reactions the most serious problem is the representation of the interaction of the solute with the solvent. This problem is particularly acute in the case of ions.

There are several general schemes for evaluating the solution energetics, including (i) a polarizable continuum model, in which the polarization of the bulk solvent by the charge distribution of the solute is evaluated; (ii) supermolecule approaches in which the solute and several explicit solvent molecules surrounding it are treated quantum mechanically; and (iii) molecular dynamic simulation techniques, in which many solvent molecules interact with the solute through pair or high-order potentials. These potentials are calculated quantum mechanically or fitted to experimental data. In the present study on aluminum−water complexes we employ a supermolecule approach. In later studies this will be combined with polarizable continuum calculations. A similar approach has been previously applied to arsenic oxide and hydroxide species (*9*).

The structures, stabilities, and vibrational spectra of aluminum−acetate complexes have been studied by Kubicki et al. (*10*). Water exchange on metal clusters has recently been studied quantum mechanically by several groups (e.g., refs *11*−*13* and *31*). These studies have been on transition metal ions, not aluminum, but several interesting facts have emerged.

First, such calculations can readily be performed for the central ion and its first hydration shell (typically 4−6 water molecules) but not with the inclusion of the complete second coordination shell (typically about 12 water molecules), although several calculations have included a single water molecule from the second coordination shell. Second, finding the actual transition states for the water exchange reaction can be quite difficult, but it is often easy to find higher symmetry intermediates, which are quite close in energy to the transition states. Third, if only the central metal ion and its five to seven nearest neighbor waters are considered, the Born and polarization energies that arise from immersion of this supermolecule into the solvent are quite large and their changes from one species to another must be considered. If the calculations are done carefully, then reasonable agreement between calculated and experimental energetics can apparently be obtained, although there is some ambiguity since several mechanisms are possible and their overall energetics are sometimes similar.

For the hexaqua and monofluoro cases we consider the six-coordinated parent [e.g., $Al(OH_2)_5F^{2+}$], the five-coordinated complex produced by removal of an inner-sphere water [e.g., $Al(OH_2)_4F^{2+}$], a six-coordinated complex with an additional water in the second coordination sphere [e.g., $Al(OH_2)_5F^{2+}\cdots(H_2O)$], a five-coordinated complex with an additional water molecule in the second coordination sphere [e.g., $Al(OH_2)_4F^{2+}\cdots(H_2O)$], and the complex involved in the dissociative-interchange mechanism [e.g., $Al(OH_2)_4F^{2+}\cdot(OH_2)_2$]. For the monohydroxyl species we present here results only for the six- and five-coordinated species.

All geometries for the monomeric species were optimized at the Hartree−Fock 6-31G* level without symmetry constraints, using the program GAMESS (*14*). For the dimeric species we used polarized versions of the relativistic effective-core-potential basis sets of Stevens et al. (*15*). Evaluations of the correlation energy at the MP2 level are in progress. For most of these species we have also evaluated ^{27}Al NMR shieldings using the 6-31G* basis set and the GIAO (gauge-including atomic orbital; *16*) method using the program GAUSSIAN94 (*17*). The Al NMR shielding has also been calculated for the dimeric species $Al_2(OH)_2(OH_2)_8^{+4}$ and $Al_2F_2(OH_2)_8^{+4}$. Born and polarization energies for these various species in solution have yet to be evaluated. We have found that various standard procedures to calculate molecular volumes for these species give widely varying effective Born radii. Thus, the scheme used by Deeth and Elding (*12*) may not be generally applicable.

Summary of the Experimental Results

Large increases in solvent-exchange rates accompany both hydroxylation and fluoridation of $Al(OH_2)_6^{3+}$(aq) (*1*, *2*). At 298 K rates of exchange of inner sphere for bulk water molecules in $AlF(OH_2)_5^{2+}$(aq) and $AlF_2(OH_2)_4^{+}$(aq) are $\sim 10^2$ and $\sim 10^4$ times more rapid, respectively, than in $Al(OH_2)_6^{3+}$(aq). Deprotonation of a single water molecule on $Al(OH_2)_6^{3+}$(aq) to form the $AlOH(OH_2)_5^{2+}$(aq) complex increases the lability of the other water ligands by a factor of $> 10^4$ (Table 1). These rates are probably accurate to within a factor of 2−3. The uncertainty in these values of k^{298}_{ex} arises largely from the extrapolation of rate data measured at high temperatures to 298 K via eqs 3−5. In particular, this extrapolation, characterized by the activation parameters $\Delta S^{\ddagger}$ and $\Delta H^{\ddagger}$, is complicated by curvature in $\ln(1/T_2)$ versus $1/T$ at low temperatures due to contributions from quadrupolar relaxation. For cases in which more than one complex gives a bound-water signal, $T_2[q]$ cannot be measured directly because it does not vary enough among complexes to allow

TABLE 2. Rate Coefficients for Exchange of Water Molecules from the Inner-Coordination Sphere of Metal Complexes to the Bulk Solution Compared with the Values for the First Hydrolysis Product[a]

complex	k_{ex}^{298} (s^{-1})	$\Delta H^{\ddagger}$ (kJ mol^{-1})	$\Delta S^{\ddagger}$ (J mol^{-1} K^{-1})	$\Delta V^{\ddagger}$ (cm^3 mol^{-1})	mechanism
$Ga(H_2O)_6^{3+}$	4.0×10^2	67.1 (±2.5)	30.1 (±7.7)	+5.0 (±0.5)	I_d
$GaOH(H_2O)_5^{2+}$(aq)	1.1×10^5	58.9		+6.2	I_d
$Fe(H_2O)_6^{3+}$(aq)	1.6×10^2	64.0 (±2.5)	12.1 (±6.7)	−5.4 (±0.4)	I_a
$FeOH(H_2O)_5^{2+}$(aq)	1.2×10^5	42.4 (±1.5)	5.3 (±4)	+7.0 (±0.5)	I_d
$Al(H_2O)_6^{3+}$(aq)	1.3	84.7 (±0.3)	41.6 (±0.9)	+5.7 (±0.2)	I_d
$AlOH(H_2O)_5^{2+}$(aq)	3.1×10^4	36.4 (±5)	−36.4 (±15)		
$Cr(H_2O)_6^{3+}$(aq)	2.4×10^{-6}	108.6 (±2.7)	11.6 (±8.6)	−9.6 (±0.1)	I_a
$CrOH(H_2O)_5^{2+}$(aq)	1.8×10^{-4}	111 (±2.5)	55.6 (±8.1)	+2.7 (±0.5)	I
$Ru(H_2O)_6^{3+}$(aq)	3.5×10^{-6}	89.8 (±4)	−48.3 (±14)	−8.3 (±2.1)	I_a
$RuOH(H_2O)_5^{2+}$(aq)	5.9×10^{-4}	95.8	14.9	+0.9	I
$Rh(H_2O)_6^{3+}$(aq)	2.2×10^{-9}	131.2 (±23)	29.3 (±26)	−4.1 (±0.6)	I_a
$RhOH(H_2O)_5^{2+}$(aq)	4.2×10^{-5}	103		+1.5	I
$Ir(H_2O)_6^{3+}$(aq)	1.1×10^{-10}	130.5 (±0.6)	2.1 (±2.1)	−5.7 (±0.5)	I_a
$Ir(OH(H_2O)_5^{2+}$(aq)	5.6×10^{-7}			+1.5	I

[a] Uncertainties are included where they were reported in the original work or in later compilations by the original authors (17, 23−28).

resolution of separate resonances at temperatures where $T_2(q)^{-1} > k_{ex}$.

There are several points to note about the activation parameters. First, the variation in rates among $Al(OH_2)_6^{3+}$(aq), $AlF(OH_2)_5^{2+}$(aq), and $AlF_2(OH_2)_4^{+}$(aq) appears largely due to differences in the $\Delta S^{\ddagger}$ values, which are not well constrained for the fluoro complexes. Values of $\Delta H^{\ddagger}$ are similar for all of these complexes, although there does appear to be a trend of decreasing $\Delta H^{\ddagger}$ with fluoride substitution. The results of Hugi-Cleary et al. (*30*) for $Al(OH_2)_6^{3+}$(aq) are the most accurate because they complemented ^{17}O NMR line-broadening measurements with an injection experiment that provided a direct, low-temperature value for k_{ex}.

Second, the $\Delta S^{\ddagger}$ values for $Al(OH_2)_6^{3+}$(aq), $AlF(OH_2)_5^{2+}$(aq), and $AlF_2(OH_2)_4^{+}$(aq) are large and positive, consistent with considerable dissociative character to solvent exchange. The $AlOH(OH_2)_5^{2+}$(aq) complex has $\Delta S^{\ddagger} < 0$, which is usually interpreted to indicate an associative character to the exchange mechanism. However, in the absence of data for $\Delta V^{\ddagger}$, it is risky to assign a mechanism of reaction. For example, the relative change in $\Delta S^{\ddagger}$ values for $Fe(OH_2)_6^{3+}$(aq) and $FeOH(OH_2)_6^{2+}$(aq) are consistent with the mechanism becoming more associative upon hydrolysis, whereas high-pressure experiments (*25*) give positive $\Delta V^{\ddagger}$ values, consistent with an I_d mechanism similar to that of other trivalent metals (Table 2).

Finally, the $\Delta H^{\ddagger}$ value for the reaction is considerably reduced upon hydroxylation, but apparently not by fluoridation; $\Delta H^{\ddagger}$ for water exchange on $AlOH(OH_2)_5^{2+}$(aq) is significantly smaller than that for $Al(OH_2)_6^{3+}$(aq). Both the absolute values of $\Delta H^{\ddagger}$ for $Al(OH_2)_6^{3+}$(aq) and $AlOH(OH_2)_5^{2+}$(aq) and their relative changes are comparable to those for $Fe(OH_2)_6^{3+}$(aq) and $FeOH(OH_2)_5^{2+}$(aq).

Computational Results

As a first step in comparing calculations to the experimental results, variations in NMR shielding of aluminum between complexes can give an indication of the appropriateness of the molecular model. The equilibrium geometries calculated for the five species associated with exchange on the monofluoro complex are shown in Figure 2. In Table 3 we present the calculated ^{27}Al NMR shieldings for the various species that are derived from six-coordinated parents, as well as the shieldings of the tetrahedral anion $Al(OH)_4^{-}$(aq). The calculated deshielding of $Al(OH)_4^{-}$(aq) compared to $Al(OH_2)_6^{3+}$(aq) is 89 ppm, compared to the value of 80 ppm typically observed for solution-state NMR. The calculated difference may change slightly when better basis sets are used, electron correlation is included, and the effect of hydration of the ions is considered, but even at the present level the agreement with experiment is reasonably good.

In absolute terms, the agreement is poorer for the fluoro complexes, although the direction and additivity are reproduced by the calculations. Akitt and Elders (*18*) report that $Al(OH_2)_5F^{2+}$ and $Al(OH_2)_4F_2^{+}$ are deshielded compared to $Al(OH_2)_6^{3+}$ by about 0.7 and 1.3 ppm, respectively, while we calculate deshieldings of 6.0 and 14.2 ppm. Faust et al. (*19*) report a deshielding compared to the $Al(OH_2)_6^{3+}$ reference with increasing pH, which they attribute to exchange with an aluminum hydroxide complex having a chemical shift of 3.5 ppm. Faust et al. (*19*) ascribe this species to the monomer $AlOH(OH_2)_5^{2+}$, for which we calculate a somewhat larger deshielding of +8.8 ppm. At higher metal concentrations, Akitt and Mann (*20*) report a peak at ~4 ppm and identify it as a dimer, that is, $Al_2(OH)_2(OH_2)_8^{4+}$, although subsequent work by this group suggests that other multimers are also present (*33*). However, the dimer can be crystallized, and its chemical shift as a sulfate salt is +2 ppm in the solid state (*32*). We optimized the geometry of this species and calculate it to be deshielded compared to $Al(OH_2)_6^{3+}$ by ~2.7 ppm, in reasonable agreement with the experimentally observed shift.

For the process of water exchange we first considered a very simple limiting dissociative mechanism in which we completely removed a water molecule from the six-coordinated species (e.g., Figure 2a) to form a five-coordinated complex (Figure 2b). We found that the water removal energy is reduced when an H_2O molecule is replaced by F^- and is reduced even more when OH^- substitutes for H_2O. The removal energies for the monofluoro and monohydroxyl cases are also substantially smaller when the water removed is in the trans position with respect to the F^- or OH^-. In the complex $Al(OH_2)_5F^{2+}$ the calculated Al−O distances are 1.953 Å for the water trans to fluoride and 1.981 Å for water in the cis positions, compared to an Al−O distance of 1.934 Å for $Al(OH_2)_6^{3+}$. This difference between cis and trans reactivities cannot be observed by NMR, which measures only the average lifetime for water in the inner-coordination sphere. The removal energies are shown in Table 4. In all cases these removal energies are much larger than the measured activation enthalpies for water exchange (Table 1).

Some simple corrections should be made that will reduce the calculated values. First, the water removed is not lost to the gas phase but enters the bulk solution, where it will be made stable by ~20 kJ mol^{-1} (*21*). The five-coordinated complex left behind also has shorter bond distances than the parent six-coordinated complex, so that its effective Born radius will be smaller and, hence, its Born stabilization

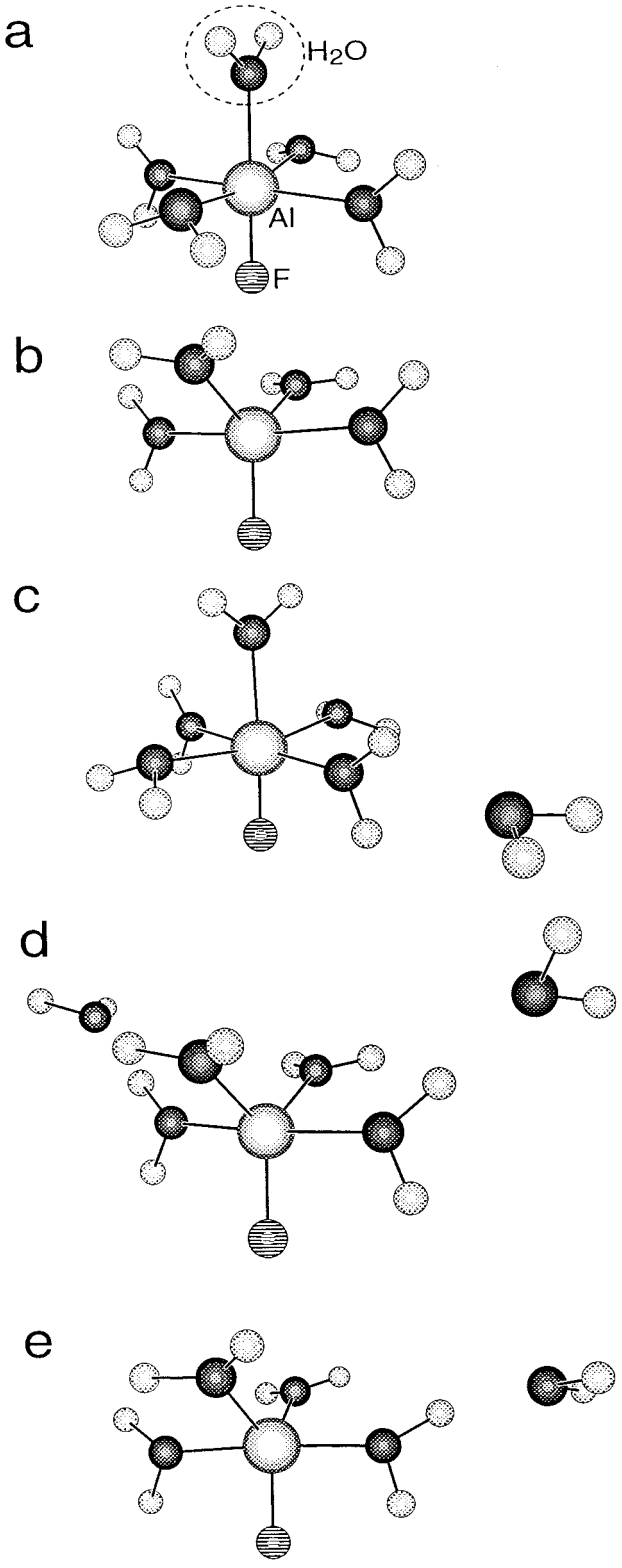

FIGURE 2. Geometries optimized at the 6-31G* SCF level for species associated with the parent $Al(OH_2)_5F^{+2}$ complex (atoms in order of decreasing size are aluminum, oxygen, fluorine, and hydrogen): (a) $Al(OH_2)_5F^{+2}$, six-coordinated parent complex; (b) $Al(OH_2)_4F^{+2}$, five-coordinated complex formed from the parent by removal of a water molecule trans to F; (c) $Al(OH_2)_5F^{+2}\cdots(OH_2)$, six-coordinated complex plus an additional water molecule in the second-coordination sphere; (d) $Al(OH_2)_4F^{+2}\cdot(OH_2)_2$, complex formed as an intermediate in the dissociative interchange (I_d) mechanism; (e) $Al(OH_2)_4F\cdots(H_2O)^{+2}$, formed by transfer of a water molecule from the first to the second coordination sphere.

TABLE 3. ^{27}Al NMR Shieldings Calculated Using the 6-31G* Basis Set, the GIAO Method, and the 6-31G* Optimized Geometries

molecular species	calcd shieldings (ppm)
$Al(OH_2)_6^{3+}$	637.3 (636.4)[a]
$Al(OH)_4^-$	548.1
$Al(OH_2)_5(OH)^{2+}$	628.5
$Al(OH_2)_4(OH)_2^+$(*cis*)	610.3
$Al(OH_2)_4(OH)_2^+$(*trans*)	612.4
$Al_2(OH)_2(OH_2)_8^{+4}$	634.6[a]
$Al(OH_2)_5F^{+2}$	631.3
$Al(OH_2)_4F_2^+$(*cis*)	623.1
$Al_2F_2(OH_2)_8^{4+}$	638.1[a]

[a] Evaluated at a geometry that was optimized using an effective core potential and the polarized SBK basis set.

TABLE 4. Calculated Energies for the Removal of a Water Molecule from Six-Coordinated Parent Complexes

species	energy to remove one H_2O (kJ mol^{-1})	relative energy[a] (kJ mol^{-1})
$Al(OH_2)_6^{3+}$	245.0	0
$Al(OH_2)_5F^{2+}$ (*cis*)	189.9	−55.0
$Al(OH_2)_5F^{2+}$ (*trans*)	163.0	−81.9
$Al(OH_2)_5OH^{2+}$ (*cis*)	166.8	−78.2
$Al(OH_2)_5OH^{2+}$ (*trans*)	148.5	−96.4

[a] Difference in energy relative to that for the $Al(OH_2)_6^{3+}$ complex.

TABLE 5. Calculated Energies for Forming a Dissociative Interchange-type Intermediate (Figure 2d) and for Forming a Second-Coordination-Sphere Complex (Figure 2e) during Exchange of H_2O for $Al(OH_2)_6^{3+}$ and $Al(OH_2)_5F^{2+}$

reaction	E_{SCF} (gas phase) (kJ mol^{-1})
Interchange Intermediates	
$Al(OH_2)_6^{3+}\cdots H_2O \rightarrow Al(OH_2)_5\cdot(H_2O)_2^{3+}$	39.0
$Al(OH_2)_5F^{2+}\cdots H_2O \rightarrow Al(OH_2)_4F\cdot(H_2O)_2^{2+}$	22.3
Second-Sphere Complexes	
$Al(OH_2)_6^{3+} \rightarrow Al(OH_2)_5^{3+}\cdots(H_2O)$	48.0
$Al(OH_2)_5F^{2+} \rightarrow Al(OH_2)_4F^{2+}\cdots(H_2O)$	54.6

consequently larger. Simply scaling the Born energy by the average Born radius calculated for the six- and five-coordinated species using the scheme of Rashin and Honig (*22*) gives an additional reduction in the removal enthalpy of ~24 kJ mol^{-1}.

One could attempt to study the five-coordinated species, such as the $Al(OH_2)_5^{3+}$, more completely within a polarizable continuum model, but such species are problematic because they are clearly unstable toward addition of a sixth water to the first coordination sphere. In any case, although the calculated removal energies do not correspond directly to the activation enthalpies for ligand exchange, their values may be related by a linear free energy relationship; for example, the enthalpy of activation for the I_d process might scale linearly with the energy for complete removal of a water molecule.

To better characterize the energetics for the water exchange process, we have considered two additional models, the energetics of which are given for the hexaqua and the monofluoro cases in Table 5. In the first case we consider reactions such as

$$AlF(OH_2)_5^{2+}\cdots H_2O \rightarrow AlF(OH_2)_4^{2+}\cdot(OH_2)_2 \qquad (8)$$

in which a second-coordination sphere water is moved

toward the metal center accompanied by lengthening of the Al−O bond to one of the inner-sphere waters, forming a dissociative interchange-like intermediate (compare panels c and d of Figure 2; see also ref *13*). The energy difference calculated for these species in the gas phase is smaller than the experimental activation energy.

An alternative reaction would be:

$$AlF(OH_2)_5^{2+} \rightarrow AlF(OH_2)_4^{2+}\cdots(H_2O) \qquad (9)$$

in which a water molecule in the first-coordination sphere is moved to the second, forming a dissociative intermediate (compare panels a and e of Figure 2). The energy for this process is also less than the experimental activation energy but somewhat closer to it. Note that for the second type of reaction the energy changes are similar for the monofluoro and hexaqua cases, consistent with experimental values (Table 1) of 85 kJ mol^{-1} for $Al(OH_2)_6^{3+}$ and 79 (±5) kJ mol^{-1} for $Al(OH_2)_5F^{2+}$. Experimentally, the difference in solvent exchange rate for these complexes is mostly an entropy effect. In principle, Born and polarization energies for the reactant and product species should then be added to obtain the reaction enthalpy in solution. However, this is a very dubious and ambiguous procedure. The magnitude of the Born energy is ∼6300 kJ mol^{-1} divided by the Born radius in angstroms for the triply charged species. Therefore, a small difference in Born radius between reactant and product can give a very large energy effect.

Overall, there are satisfying agreements between the calculations and experimental data. Experimentally, substitution of hydroxide or fluoride ion into the inner-coordination sphere of $Al(OH_2)_6^{3+}$ labilizes the remaining inner-sphere water molecules. The magnitude of this labilization is unequivocal, but $\Delta H^{\ddagger}$ and $\Delta S^{\ddagger}$ are more uncertain because of difficulties determining the quadrupolar contribution to the line width when more than one species is present. Furthermore, assignment of mechanism requires $\Delta V^{\ddagger}$ values from variable-pressure experiments; the experimental $\Delta S^{\ddagger}$ values are too small and uncertain to infer the exchange mechanism.

Theoretical calculations, on the other hand, show that introduction of hydroxide or fluoride ion into the inner-coordination sphere greatly reduces the energy for removing a water molecule. The energies are sensitive to the location of ligand substitution, which suggests a potentially powerful tool for constraining reaction stoichiometries. Not surprisingly, the calculated energy differences are much larger than the measured activation enthalpies, which indicates the importance of interaction with second-sphere and bulk solvent molecules. Comparisons with the experimental energies are more reasonable when the second-sphere water molecules are included, as one expects for an aqueous interchange reaction. Future work should focus on the role of these second-sphere waters.

Acknowledgments

We thank Drs. D. J. Sullivan and J. Nordin for help, advice, and use of their data for Figure 1b. Support for this research was from U.S. NSF Grants EAR 96-25663, 94-14103 (to W.H.C.) and U.S. DOE Grants DE-FG03-96ER14629 (to B.L.P. and W.H.C.) and DE-FG02-94ER14467 to (to J.A.T.).

Literature Cited

(1) Phillips, B. L.; Casey, W. H.; Crawford, S. N. *Geochim. Cosmochim. Acta* **1997**, *61*, 3041−3049.
(2) Nordin, J. P.; Sullivan, D. J.; Phillips, B. L.; Casey, W. H. *Inorg. Chem.* In press.
(3) Harris, R. K. *Nuclear Magnetic Spectroscopy: A Physicochemical View*; Longman Scientific and Technical: New York, 1986; pp 81−88, 127−129.
(4) Hehre, W. J.; Radom, L.; Schleyer, P. V. R.; Pople, J. A. *Ab Initio Molecular Orbital Theory*; Wiley: New York, 1986.
(5) Foresman, J. B.; Frisch, A. *Exploring Chemistry with Electronic Structure Methods*, 2nd ed.; GAUSSIAN Inc.: Pittsburgh, PA, 1995.
(6) Pople, J. A.; Binkley, J. S.; Seeger, R. *Int. J. Quantum Chem. Symp.* **1976**, *10*, 1−22.
(7) Cramer, C. J.; Elding, L. I. *Structure and Reactivity in Aqueous Solution: Characterization of Chemical and Biological Systems*; ACS Symposium Series 568; American Chemical Society: Washington, DC, 1994.
(8) Wiberg, K. B.; Castejon, H.; Keith, T. A. *J. Comput. Chem.* **1996**, *17*, 185−190.
(9) Tossell, J. A. *Geochim. Cosmochim. Acta* **1997**, *61*, 1613−1623.
(10) Kubicki, J. D.; Blake, G. A.; Apitz, S. E. *Geochim. Cosmochim. Acta* **1996**, *60*, 4897−4911.
(11) Bleuzen, A.; Foglia, F.; Fuet, E.; Helm, L.; Merbach, A. E.; Weber, J. *J. Am. Chem. Soc.* **1996**, *118*, 12777−12787.
(12) Deeth, R. J.; Elding, L. I. *Inorg. Chem.* **1996**, *35*, 5019−5026.
(13) Rotzinger, F. P. *J. Am. Chem. Soc.* **1996**, *118*, 6760−6766.
(14) Schmidt, M. W.; Baldridge, K. K.; Boatz, J. A.; Elbert, S. T.; Gordon, M. S.; Jensen, J. H.; Koseki, S.; Matsunaga, N.; Nguyen, K. A.; Su, S. J.; Windus, T. L.; Dupuis, M.; Montgomery, J. A. *J. Comput. Chem.* **1993**, *154*, 1347−1363.
(15) Stevens, W. J.; Krauss, M.; Basch, H.; Jansen, P. G. *Can. J. Chem.* **1992**, *70*, 612−630.
(16) Wolinski, K.; Hinton, J. F.; Pulay, P. *J. Am. Chem. Soc.* **1990**, *112*, 8251−8260.
(17) Frisch, J. J. GAUSSIAN94, rev. B.3; Gaussian Inc.: Pittsburgh, PA.
(18) Akitt, J. W.; Elders, J. M. *J. Chem. Soc., Faraday Trans. 1* **1985**, *81*, 1923−1930.
(19) Faust, B. C.; Labiosa, W. B.; Dai, K. O.; MacFall, J. S.; Browne, B. A.; Ribeiro, A. A.; Richter, D. D. *Geochim. Cosmochim. Acta* **1995**, *59*, 2651−2661.
(20) Akitt, J. W.; Mann, B. E. *J. Magn. Reson.* **1981**, *44*, 584−589.
(21) Krauss, M.; Garmer, D. L. *J. Am. Chem. Soc.* **1991**, *113*, 6426−6435.
(22) Rashin, A. A.; Honig, B. *J. Phys. Chem.* **1985**, *89*, 5588−5593.
(23) Cusanelli, A.; Frey, U.; Richens, D. T.; Merbach, A. E. *J. Am. Chem. Soc.* **1996**, *118*, 5265−5271.
(24) Rapaport, I.; Helm, L.; Merbach, A. E.; Bernhard, P.; Ludi, A. *Inorg. Chem.* **1988**, *27*, 873−879.
(25) Swaddle, T. W.; Merbach, A. E. *Inorg. Chem.* **1981**, *20*, 4212−4216.
(26) Hugi-Cleary, D.; Helm, L.; Merbach, A. E. *J. Am. Chem. Soc.* **1987**, *109*, 4444−4450.
(27) Xu, F.-C.; Krouse, H. R.; Swaddle, T. W. *Inorg. Chem.* **1985**, *24*, 267−270.
(28) Laurenczy, G.; Rapaport, I.; Zbinden, D.; Merbach, A. E. *Magn. Reson. Chem.* **1991**, *29*, S45−51.
(29) Merbach, A. E. *Pure Appl. Chem.* **1982**, *54*, 1479−1493.
(30) Hugi-Cleary, D.; Helm, L.; Merbach, A. E. *Helv. Chim. Acta* **1985**, *68*, 545−554.
(31) Tsutsui, Y.; Wasada, H.; Funahashi, S. *Bull. Chem. Soc. Jpn.* **1997**, *70*, 1813−1825.
(32) Thompson, A. R.; Kunwar, A. C.; Gutowsky, H. S.; Oldfield, E. *J. Chem. Soc., Dalton Trans.* **1987**, 2317.
(33) Akitt, J. W.; Elders, J. M. *J. Chem. Soc., Dalton Trans.* **1988**, 1347.

Received for review March 9, 1998. Revised manuscript received June 1, 1998. Accepted June 15, 1998.

ES9802246